Synchronous chaos in coupled oscillator systems

J. F. Heagy, T. L. Carroll, and L. M. Pecora
Material Science Division, Naval Research Laboratory, Washington, D.C. 20375-5000
(Received 28 March 1994)

We investigate the synchronization of chaotic oscillations in coupled oscillator systems, both theoretically and in analog electronic circuits. Particular attention is paid to deriving and testing general conditions for the stability of synchronous chaotic behavior in cases where the coupled oscillator array possesses a shift-invariant symmetry. These cases include the well studied cases of nearest-neighbor diffusive coupling and all-to-all or global coupling. An approximate criterion is developed to predict the stability of synchronous chaotic oscillations in the strong coupling limit, when the oscillators are coupled through a single coordinate (scalar coupling). This stability criterion is illustrated numerically in a set of coupled Rössler-like oscillators. Synchronization experiments with coupled Rössler-like oscillator circuits are also carried out to demonstrate the applicability of the theory to real systems.

PACS number(s): 05.45.+b, 84.30.Wp

I. INTRODUCTION

Coupled dynamical systems are typically synthesized from simpler, low-dimensional systems to form new and more complex systems. This is often done with the intent of realistically modeling spatially extended systems, with the belief that dominant features of the underlying constituents will be retained. From an applications point of view this building up approach can also be used to create a novel system whose behavior is more flexible or richer than that of the constituents, but whose analysis and/or control remains tractable. These and other motivations have led to numerous studies of coupled systems in a wide range of disciplines. Even an abbreviated list of coupled oscillator references is prohibitively long; representative works are in optical [1–4], chemical [5–7], condensed matter [8,9], biological [10–14], neural network [15–18], and other [19–22] systems.

Synchronization has long been of interest in systems of identical or nearly identical coupled subsystems. The phenomenon of synchronization of coupled *chaotic* systems has recently become a topic of great interest, and is the focus of the present work. Systems that display this behavior are temporally chaotic, but spatially ordered or *coherent*. Here the coherence is of a particular type—the dynamics is the same or nearly so for long periods of time for all coupled subsystems or large regions of them.

Standard approaches to the study of coherent chaotic oscillations fall into a few broad categories. First is the analysis of small numbers of coupled systems, typically two to four [23–25], where analytic methods can be applied. For large systems, where analytic methods are lacking, intensive numerical studies are often the only recourse. Coupled map lattice models [26–30] have received considerable attention and offer a third, middle ground between these extremes. One drawback of coupled map lattice models, however, is the general inability to relate their quantitative features to the measurable properties of real physical systems. There is a need for unifying existing work and extending analytic methods to large assemblies of interacting nonlinear oscillators.

There are a few exceptions to these approaches. One noteworthy early work on synchronized chaotic oscillations is the paper by Fujisaka and Yamada [31]. They consider a spatially one-dimensional, diffusively coupled system composed of identical, possibly chaotic oscillators. The boundary conditions are either periodic or open ended. Fujisaka and Yamada derive general conditions for the stability of the synchronized state using previous results for determinants of matrices with structure arising from nearest-neighbor coupling [32–34]. Their conditions are based on solutions of a set of low-dimensional variational equations, typically the dimension of an individual oscillator, rather than on solutions of the full variational equations in the synchronized state.

Another work relevant to the present study is the paper by Shnöl [35]. The focus of this paper is on the stability of synchronous *periodic* oscillations, however the results also apply to synchronous chaotic oscillations. Shnöl studied the situation where all oscillators are coupled equally through a medium which has its own dynamics. This is a form of all-to-all or global coupling. Shnöl showed that the stability of the synchronized state can be determined by solving a set of low-dimensional variational equations.

The basic synchronization problem can be framed with the questions, "will my system ever synchronize and, if so, under what conditions?" In this work we provide partial answers to these questions for a restricted, but representative class of coupled dynamical systems—those that exhibit *shift-invariant symmetry*. Shift-invariant symmetry is a property shared by many commonly studied coupled oscillator systems, notably those with nearest-neighbor diffusive coupling and global coupling.

In general, the synchronization problem can be broken down into two distinct subproblems. The first (macro) problem is to reduce a high-dimensional set of variational equations, governing the stability of the synchronous state, to a more manageable, low-dimensional set. Cen-

tral to this reduction is the idea of *synchronization manifold,* on which synchronized dynamics is constrained. The stability of the synchronized state is insured if variations *transverse* to this manifold decay with time (variations *within* the synchronization manifold do not affect the stability of the synchronized state). For systems with shift-invariant symmetry the variational equations can always be transformed to a new representation where the transverse and nontransverse variations decompose naturally; a convenient transformation is the (spatial) discrete Fourier transform. Only the transverse variational equations need to be considered to address stability questions, and these equations typically come in independent, low-dimensional sets (usually the dimension of a single oscillator). Often the reduced sets have similar or identical structure and stability can be ascertained by studying a single set. A general procedure for carrying out this decomposition for shift-invariant symmetry is developed in Sec. II. This procedure allows one to directly and easily derive the reduced variational equations for many special cases. In particular, the results of Fujisaka and Yamada and of Shnöl are immediately obtained, as shown in Sec. III. Moreover, the procedure provides a general framework for analyzing a large class of coupled oscillator systems. In the Appendix we outline an extension of the procedure to handle a particular case with *free-end* boundary conditions.

The second (micro) problem is to compute the Lyapunov exponents of the transverse variational equations to determine their stability. For certain special cases, notably when the coupling between oscillators is through all coordinates (vector coupling), the Lyapunov exponents of the transverse variational equations can be easily related to the Lyapunov exponents of a single, isolated oscillator. Typically this is not the case and there is no general procedure (known to us) for predicting the Lyapunov exponents, or even the largest Lyapunov exponent, of the transverse variational equations. A case that is expected to arise frequently in practice is that of *scalar coupling,* where the oscillators are coupled via a single coordinate. This case cannot be treated exactly, however, in the limit of large coupling an approximate analysis can be carried out via perturbation theory. This analysis, which is developed in Sec. III, yields a straightforward and easily implemented stability criterion for synchronous chaotic oscillations. This stability condition is similar to the condition for chaotic synchronization in "one-way" driving cases developed in [36,37].

In Sec. IV we explore the stability of synchronous chaotic oscillations numerically and experimentally in coupled chaotic electronic circuits. Each circuit is a simple, but robust Rössler-like [38] oscillator that can be duplicated fairly accurately. These circuits serve well as individual chaotic subsystems and can be easily coupled to other Rössler-like circuits to produce synchronous chaos. Numerical simulations of the coupled Rössler-like circuit configurations are also carried out and compared to the experimental results. The large scalar coupling predictions of Sec. III are tested and verified numerically for all possible scalar coupling choices.

In Sec. V we summarize our main results.

II. SYSTEMS UNDER STUDY

We are interested in studying systems of nonlinear oscillators that are coupled together in some regular fashion. In this study we shall deal mainly with N identical coupled oscillators that can be represented by a dynamical system of the form

$$\begin{aligned}
\frac{dx^0}{dt} &= F(x^0)+cG^0(x^0,x^1,\ldots,x^{N-1}) ,\\
\frac{dx^1}{dt} &= F(x^1)+cG^1(x^0,x^1,\ldots,x^{N-1}) ,\\
&\vdots \\
\frac{dx^{N-1}}{dt} &= F(x^{N-1})+cG^{N-1}(x^0,x^1,\ldots,x^{N-1}) .
\end{aligned} \tag{1}$$

Here the x^i are individual oscillator coordinates, $x^i=(x^i_1,x^i_2,\ldots,x^i_n)\in\mathbb{R}^n$, and F: $\mathbb{R}^n\to\mathbb{R}^n$ is the (nonlinear) vector field controlling the dynamics of a single oscillator. The functions G^i: $\mathbb{R}^m\to\mathbb{R}^n$, where $m=nN$, describe the coupling of the ith oscillator to all other oscillators and c is a scalar coupling constant. We restrict the coupling functions G^i so that they vanish when the oscillators are synchronized; $G^i(x(t),x(t),\ldots,x(t))\equiv 0$, $i=0,\ldots,N-1$. This ensures that any solution $x(t)$ for a single oscillator is also a solution of the coupled system (1).

The coupling functions come in two general varieties, shift-invariant and non-shift-invariant. For shift-invariant cases the coupling configuration does not vary from one oscillator to the next; the oscillators can be considered to occupy points on a one-dimensional lattice with periodic boundary conditions, or equivalently on a ring with N sites. The shift-invariance of the coupling is expressed algebraically as

$$\begin{aligned}
&G^i(x^j,x^{j+1},\ldots,x^{j+N-1}) \\
&\qquad = G^{i+1}(x^{j-1},\ x^j,\ldots,x^{j+N-2}) ,
\end{aligned} \tag{2}$$

for $i,j=0,1,\ldots,N-1$, where all indices are understood to be taken mod N (extensions to two and higher-dimensional lattices are possible, but will not be considered explicitly here). A common example of shift-invariant coupling is nearest-neighbor diffusive coupling, for which $G^i=x^{i-1}-2x^i+x^{i+1}$. Another common example of shift-invariant coupling is so-called all-to-all or global coupling, which typically has the form

$$G^i=\frac{1}{N}\sum_{k=0}^{N-1} g(x^k-x^i) . \tag{3}$$

Here g is a vector function satisfying $g(0)=0$. Each of these coupling cases will be considered in more detail below.

Common examples of non-shift-invariant coupling are nearest-neighbor coupling cases with fixed- or free-end conditions; these cases do not satisfy condition (2). We mainly consider shift-invariant coupling in this paper, although our results can be extended to a nearest-neighbor case with free-end boundary conditions (see Appendix).

A central goal of this study is the ability to predict

when the synchronized state defined by $s(t)=x^0=x^1=\cdots=x^{N-1}$ is stable. In what follows we present the stability analysis for shift-invariant coupling. The starting point in this analysis is the linearization of system (1) about the synchronized state $s(t)$. This leads to a set of linear variational equations given by

$$\frac{d\xi^i}{dt}=DF(s)\xi^i+c\sum_{j=0}^{N-1}D_jG^i(x^0,x^1,\ldots,x^{N-1})|_s\xi^j\,,\quad i=0,1,\ldots,N-1 \tag{4}$$

where $\xi^i=x^i-s(t)$, $DF(s)$ is the Jacobian of the vector field F evaluated on $s(t)$, and D_j is the differential operator acting on coordinates of the jth oscillator. Since the coupling is shift-invariant relation (2) can be used to express all of the derivatives $D_jG^i(x^0,x^1,\ldots,x^{N-1})|_s$ in terms of derivatives of $G^0(x^0,x^1,\ldots,x^{N-1})$. The result is

$$\frac{d\xi^i}{dt}=DF(s)\xi^i+c\sum_{j=0}^{N-1}D_{j-i}G^0(x^0,x^1,\ldots,x^{N-1})|_s\xi^j\,. \tag{5}$$

These equations can be placed in the form of a discrete circular convolution by defining the "backward" sequence

$$\{H^i\}_{i=0}^{N-1}=\{DF(s)+cD_0G^0|_s,cD_{N-1}G^0|_s,cD_{N-2}G^0|_s,\ldots,cD_1G^0|_s\}\,. \tag{6}$$

The variational equations then become

$$\frac{d\xi^i}{dt}=\sum_{j=0}^{N-1}H^{i-j}\xi^j,\quad i=0,1,\ldots,N-1\,. \tag{7}$$

By introducing discrete Fourier transforms of the sequence (6) and the sequence $\{\xi^0,\xi^1,\ldots,\xi^{N-1}\}$,

$$Y^k=\frac{1}{\sqrt{N}}\sum_{j=0}^{N-1}H^je^{2\pi ijk/N}\,, \tag{8a}$$

$$\eta^k=\frac{1}{\sqrt{N}}\sum_{j=0}^{N-1}\xi^je^{2\pi ijk/N}\,, \tag{8b}$$

the convolution (7) is block-diagonalized by virtue of the convolution theorem for discrete Fourier transforms [39]. The transformed variational equations are given by

$$\frac{d\eta^k}{dt}=\sqrt{N}\,Y^k\eta^k,\quad k=0,1,\ldots,N-1\,. \tag{9}$$

Note that the Fourier transform diagonalization method can be applied to *any* set of coupled systems represented by equations of the form

$$\frac{dx^i}{dt}=f^i(x^0,x^1,\ldots,x^{N-1}),\quad i=0,1,\ldots,N-1 \tag{10}$$

that satisfy the shift-invariance conditions

$$f^i(x^j,x^{j+1},\ldots,x^{j+N-1})=f^{i+1}(x^{j-1},x^j,\ldots,x^{j+N-2})\,; \tag{11}$$

it is not necessary for the ith equation to be decomposable into oscillator plus coupling. The coupled van der Pol oscillator problem considered in [40] is one example.

Before proceeding, it is useful to discuss the geometry of the variations η^k. The dynamical system (1) evolves in $\mathbb{R}^m$, where $m=nN$. The *synchronization manifold*, $\mathcal{M}\subset\mathbb{R}^m$, is defined by the conditions $x^0=x^1=\cdots=x^{N-1}$. Synchronous solutions of all types (not just chaotic solutions) are constrained to this manifold (hyperplane). The synchronization conditions represent $n(N\text{-}1)$ constraint equations. Therefore the dimension of $\mathcal{M}$ is $nN-n(N-1)=n$, which is the phase space dimension of a single oscillator. The Fourier transform basis η^k provides a convenient decomposition of the variations into variations *within* $\mathcal{M}$ and variations *transverse* to $\mathcal{M}$. Note that the vector $e=\sum_{i=0}^{N-1}x^i$ is within the synchronization manifold. It follows from (8b) that the variation η^0 is parallel to e and is therefore within $\mathcal{M}$. The remaining variations $\eta^k,k=1,2,\ldots,N-1$, are transverse to $\mathcal{M}$ and control the stability of the synchronized state [41]. Stability of the synchronized state is insured if arbitrary small transverse variations decay to zero.

In some cases the variation η^0 obeys the variational equation for a single, isolated oscillator. This occurs whenever the coupling functions satisfy the constraint

$$\sum_{j=0}^{N-1}G^j(x^0,x^1,\ldots,x^{N-1})=\text{const}\,, \tag{12}$$

as shown below. This is a common constraint and holds for nearest-neighbor diffusive coupling and global coupling of the form (3) whenever the function g is odd. Typically the constant in (12) is zero. From (6), (8a), and (9) η^0 satisfies

$$\frac{d\eta^0}{dt}=\left[DF(s)+c\sum_{j=0}^{N-1}D_jG^0(x^0,x^1,\ldots,x^{N-1})|_s\right]\eta^0\,. \tag{13}$$

We must show that the sum in (13) vanishes as a result of the constraint (12). To do this first differentiate (12) with respect to the zeroth oscillator coordinates and evaluate the result on s. One obtains

$$\sum_{j=0}^{N-1}D_0G^j(x^0,x^1,\ldots,x^{N-1})|_s=0\,. \tag{14}$$

Applying the shift-invariance relation (2) yields

$$\sum_{j=0}^{N-1}D_{N-j}G^0(x^0,x^1,\ldots,x^{N-1})|_s=0\,. \tag{15}$$

This sum is over all oscillators and is therefore equivalent to the sum in (13). This proves the relation and the variational equation for η^0 becomes

$$\frac{d\eta^0}{dt}=DF(s)\eta^0 , \tag{16}$$

which is recognized as the variational equation used to compute the Lyapunov exponents of a single oscillator exhibiting the solution $s(t)$.

The Lyapunov exponents are computed from the time evolution operator for the variation η^0, defined by

$$\eta^0(t)=\Lambda^0(t)\eta^0(0) , \tag{17a}$$

$$\Lambda^0(0)=1 . \tag{17b}$$

$\Lambda^0(t)$ satisfies (16) with $\eta^0(t)$ replaced by $\Lambda^0(t)$, and has the solution

$$\Lambda^0(t)=T\exp\left[\int_0^t J(t')dt'\right] , \tag{18}$$

where $J(t)=DF(s(t))$ and T is the time ordering operator. Let $\mu_i^0(t)$, $i=1,\ldots,n$ be the eigenvalues of $\Lambda^0(t)$. The Lyapunov exponents of (16) are then given by

$$\lambda_i^0=\mathrm{Re}\lim_{t\to\infty}\frac{1}{t}\ln\mu_i^0(t),\quad i=1,\ldots,n . \tag{19}$$

These Lyapunov exponents determine the nature of the synchronized state in the usual way. In particular, a positive Lyapunov exponent implies chaotic behavior.

As mentioned earlier, the transverse variations η^k, $k=1,2,\ldots,N-1$ control the stability of the synchronized state. Any deviation from the synchronization manifold will be reflected in the growth of one or more of these variations. Combining (8a) and (9) the transverse variations satisfy

$$\frac{d\eta^k}{dt}=\left[\sum_{j=0}^{N-1}H^j e^{2\pi ijk/N}\right]\eta^k,\quad k=1,\ldots,N-1 . \tag{20}$$

Let $\Lambda^k(t)$ be the time evolution operator of the kth transverse variation and let $\mu_i^k(t)$, $i=1,\ldots,n$, be the eigenvalues of $\Lambda^k(t)$. The *transverse Lyapunov exponents are defined by*

$$\lambda_i^k=\mathrm{Re}\lim_{t\to\infty}\frac{1}{t}\ln\mu_i^k(t),\quad i=1,\ldots,n,\quad k=1,\ldots,N-1 \tag{21}$$

(transverse Lyapunov exponents have also been utilized in other works [42–44]). Let $\lambda_{\max}$ be the largest transverse Lyapunov exponent. The synchronized state s is stable (unstable) for $\lambda_{\max}<0$ ($\lambda_{\max}>0$). Unfortunately, not much more can be said about the transverse variational equations (20) for arbitrary coupling choices. For this reason we turn our attention to specific cases.

III. SPECIFIC COUPLING CASES

A. Diffusive coupling: vector case

A common form of shift-invariant coupling is nearest-neighbor diffusive coupling, given by $G^i=x^{i-1}-2x^i+x^{i+1}$. This coupling derives its name from its close connection to the Laplacian operator ∇^2; G^i is the discrete (centered-difference) representation of $\nabla^2 x(r)$, where r is a spatial coordinate (cf., [45]). Here we consider a slight generalization of diffusive coupling where each component of $x^{i-1}-2x^i+x^{i+1}$ is multiplied by an arbitrary coefficient

$$G^i=\Gamma(x^{i-1}-2x^i+x^{i+1}) , \tag{22a}$$

$$\Gamma=\mathrm{diag}(\gamma_1,\gamma_2,\ldots,\gamma_n) . \tag{22b}$$

For now we assume $\gamma_i>0$, $i=1,\ldots,n$. Below we take up the case where one or more coefficients γ_i is zero. From (6) and (20) the transverse variational equations for diffusive coupling are given by

$$\begin{aligned}\frac{d\eta^k}{dt}&=[DF(s)-2c\Gamma+c\Gamma e^{2\pi ik/N}+c\Gamma e^{2\pi i(N-1)k/N}]\eta^k\\&=\left[DF(s)-4c\sin^2\left[\frac{\pi k}{N}\right]\Gamma\right]\eta^k ,\\&\qquad k=1,2,\ldots,N-1 ,\end{aligned} \tag{23}$$

where the last relation follows from a trigonometric half-angle relation. This result has also been obtained by Fujisaka and Yamada [31]. In the special case for which all of the γ_i are equal we can absorb γ_i into the coupling constant c and set $\Gamma=1$. Since $DF(s(t))=J(t)$ commutes with the identity matrix for all times t, the time evolution operator $\Lambda^k(t)$ factors according to

$$\Lambda^k(t)=\Lambda^0(t)\exp\left[-4c\sin^2\left[\frac{\pi k}{N}\right]t\right] . \tag{24}$$

It follows that the transverse Lyapunov exponents are given by

$$\lambda_i^k=\lambda_i^0-4c\sin^2\left[\frac{\pi k}{N}\right],\quad k=1,2,\ldots,N-1 \tag{25}$$

from which $\lambda_{\max}=\lambda_{\max}^0-4c\sin^2(\pi/N)$. It is therefore possible to have stable synchronized chaotic solutions, provided the coupling constant c is large enough. As c is reduced the mode with the longest "spatial wavelength," η^1, is the first to lose stability.

B. Diffusive coupling: scalar case

Scalar diffusive coupling, for which there is a single nonzero entry in the diagonal matrix Γ, is perhaps the simplest form of coupling and the easiest to implement experimentally (see Sec. IV below). Nevertheless, the stability analysis for this case cannot be carried out exactly. Without loss of generality we can choose the nonzero entry of Γ to be $\gamma_1\equiv 1$. Again we are interested in determining conditions under which the synchronized state s is stable. Here we present an approximate theory whose aim is to find these conditions in the limit of large coupling. We first redefine the time in the variational equations (23):

$$\tau=4c\sin^2\left[\frac{\pi k}{N}\right]t . \tag{26}$$

The transverse variational equations then become

$$\frac{d\eta}{d\tau}=[-\Gamma+\varepsilon DF(s)]\eta \ , \tag{27}$$

with $\varepsilon=[4c\sin^2(\pi k/N)]^{-1}$ (the explicit k dependence of the variations is suppressed in the following development). In this representation, for large c the Jacobian $DF(s)$ is a perturbation to the matrix Γ. Let Λ be the evolution operator of the variation η; Λ satisfies (27) with η replaced by Λ. We seek Λ to leading order in ε. This is facilitated by factoring Λ as follows:

$$\Lambda=UQ \ , \tag{28}$$

where U is the time evolution operator of (27) for $\varepsilon=0$ (infinite coupling limit):

$$U=\exp(-\Gamma\tau)=\mathrm{diag}[\exp(-\tau),1,1,\ldots,1] \ . \tag{29}$$

Substituting (28) into (27) yields an equation for the operator Q:

$$\frac{dQ}{d\tau}=\varepsilon U^{-1}DF(s)UQ \ . \tag{30}$$

This is equivalent to the integral equation

$$Q(\tau)=\mathbf{1}+\varepsilon\int_0^\tau U^{-1}DF(s)UQ\,d\tau' \ , \tag{31}$$

which can be formally solved by iteration. To order ε the solution is

$$Q(\tau)=\mathbf{1}+\varepsilon\int_0^\tau U^{-1}DF(s)U\,d\tau' \ , \tag{32}$$

and therefore from (28) the evolution operator is

$$\Lambda(\tau)\approx U(\tau)\left[\mathbf{1}+\varepsilon\int_0^\tau U^{-1}DF(s)U\,d\tau'\right] \ . \tag{33}$$

The stability of the synchronized state is determined by the eigenvalue of Λ having the largest real part. For small ε (large coupling) we expect the eigenvector corresponding to this eigenvalue to lie near the eigenvector of U having the largest eigenvalue. The eigenvalues of U are simply $\{\exp(-\tau),1,1,\ldots,1\}$ and the corresponding eigenvectors form the standard basis in $\mathbb{R}^n$, denoted by $\{u_i\}$, $i=1,2,\ldots,n$. Thus the largest eigenvalue 1 is $n-1$ fold degenerate and belongs to the subspace spanned by the orthogonal complement of u_1. Let this subspace be denoted by $\mathcal{E}$. We seek the largest eigenvalue of Λ via (degenerate) first order perturbation theory [46]:

$$\begin{aligned}&\Lambda(\tau)\psi(\tau)=\mu(\tau)\psi(\tau) \ ,\\ &[U(\tau)+\varepsilon W(\tau)][\chi+\varepsilon\phi(\tau)]=[1+\varepsilon\sigma(\tau)][\chi+\varepsilon\phi(\tau)] \ ,\end{aligned} \tag{34}$$

where

$$W(\tau)=U(\tau)\int_0^\tau U^{-1}DF(s)U\,d\tau' \ , \tag{35}$$

and χ is a vector in the subspace $\mathcal{E}$. The order ε term in (34) yields the equation

$$[U(\tau)-1]\phi(\tau)+[W(\tau)-\sigma(\tau)]\chi=0 \ . \tag{36}$$

Define the projection operator onto the subspace $\mathcal{E}$:

$$P=\sum_{i=2}^{n}u_i^T u_i \ . \tag{37}$$

Operating on the left of (36) with P gives

$$P[W(\tau)-\sigma(\tau)]\chi=0 \ . \tag{38}$$

Since $P\chi=\chi$ this equation can be written as

$$\hat{W}(\tau)\chi=\sigma(\tau)\chi \ , \tag{39}$$

where $\hat{W}(\tau)$ is the restriction of $W(\tau)$ to $\mathcal{E}$:

$$\hat{W}(\tau)=PW(\tau)P \ . \tag{40}$$

Equation (39) is an eigenvalue equation acting entirely within the subspace $\mathcal{E}$. A straightforward calculation shows that the matrix $\hat{W}(\tau)$ is given by

$$\begin{aligned}\hat{W}(\tau)&=P\int_0^\tau DF(s(\tau'))d\tau' P\\ &\approx\tau P\langle DF(s)\rangle P\\ &=\tau\begin{bmatrix}\left\langle\frac{\partial F_2}{\partial x_2}\right\rangle & \left\langle\frac{\partial F_2}{\partial x_3}\right\rangle & \cdots & \left\langle\frac{\partial F_2}{\partial x_n}\right\rangle\\ \left\langle\frac{\partial F_3}{\partial x_2}\right\rangle & \left\langle\frac{\partial F_3}{\partial x_3}\right\rangle & \cdots & \left\langle\frac{\partial F_3}{\partial x_n}\right\rangle\\ \vdots & \vdots & \ddots & \vdots\\ \left\langle\frac{\partial F_n}{\partial x_2}\right\rangle & \left\langle\frac{\partial F_n}{\partial x_3}\right\rangle & \cdots & \left\langle\frac{\partial F_n}{\partial x_n}\right\rangle\end{bmatrix} \ ,\end{aligned} \tag{41}$$

where $\langle\ \rangle$ denotes time average. The matrix in (41) is simply the average sub-Jacobian of F corresponding to the coordinates $x_2,x_3,\ldots,x_n$.

Let $\rho_{\max}$ be the eigenvalue of the average sub-Jacobian having the largest real part. From (39) and (41) it follows that $\sigma_{\max}=\rho_{\max}\tau$. Then the largest Lyapunov exponent of Λ is given approximately by

$$\begin{aligned}\lambda_{\max}&=\mathrm{Re}\lim_{\tau\to\infty}\frac{1}{\tau}\ln\mu(\tau)=\mathrm{Re}\lim_{\tau\to\infty}\frac{1}{\tau}\ln(1+\varepsilon\rho_{\max}\tau)\\ &=\mathrm{Re}(\varepsilon\rho_{\max}) \ .\end{aligned} \tag{42}$$

Therefore the stability of synchronized oscillations for large scalar diffusive coupling is governed by the condition $\mathrm{Re}(\rho_{\max})<0$ (assuming positive coupling constant). This result should be considered as more of a guide to answering the question, "Will the system synchronize for large coupling?", than as an accurate estimate of the largest Lyaunpov exponent of the transverse variations. Nonetheless, as shown in Sec. IV below, this criterion is capable of providing good qualitative and reasonable quantitative predictions of the largest transverse Lyapunov exponent in numerical experiments.

It has been pointed out by Rabinovich [47] that earlier work on two coupled, synchronized chaotic systems [24,48,49] and driven, synchronized chaotic systems [36,37,50–58] should be related, for example, when one system's coupling parameter is pushed to an infinite value. This relation suggests that synchronization conditions similar to those on the conditional Lyapunov exponents of chaotically driven subsystems should be available for the general case of coupled systems. In fact, the stability criterion derived above is quite similar to the condition for chaotic synchronization for "one-way driv-

ing" discussed in [36,37]. The reason is that for large c the diffusively coupled system is effectively being *driven* by the coupling variable x_1.

C. Global coupling

Global coupling occurs frequently in studies of Josephson junction arrays [59–63], coupled solid-state lasers [2–4], and neural network models [18,64]. Here we discuss two types of global coupling. First we consider global coupling of the form (3)

$$G^i(x^0,x^1,\ldots,x^{N-1})=\frac{1}{N}\sum_{k=0}^{N-1} g(x^k-x^i)\ . \tag{43}$$

In this case the matrix sequence $\{H^i\}_{i=0}^{N-1}$ in (6) is given by

$$\{H^i\}_{i=0}^{N-1}=\left\{DF(s)-\frac{c(N-1)}{N}Dg(0),\frac{c}{N}Dg(0),\frac{c}{N}Dg(0),\ldots,\frac{c}{N}Dg(0)\right\}, \tag{44}$$

and from (20) the transverse variational equations are given by

$$\frac{d\eta^k}{dt}=\left[DF(s)-cDg(0)+\frac{c}{N}Dg(0)\sum_{j=0}^{N-1}e^{2\pi ijk/N}\right]\eta^k\ . \tag{45}$$

For $k\neq 0$ (the transverse modes) the sum in (45) vanishes, leaving simply

$$\frac{d\eta^k}{dt}=[DF(s)-cDg(0)]\eta^k,\quad k=1,2,\ldots,N-1\ . \tag{46}$$

This equation has the same form as Eq. (23) above. If $Dg(0)$ is a multiple of the identity, $Dg(0)=\gamma 1$, the transverse Lyapunov exponents are given by

$$\lambda_i^k=\lambda_i^0-c\gamma,\quad k=1,2,\ldots,N-1\ . \tag{47}$$

For scalar global coupling, for which $Dg(0)$ has a single nonzero component, and for large coupling constant c, the results of Sec. III B can be applied to determine the stability of the synchronized state. Note that, regardless of the choice of g, all of the modes η^k lose stability *simultaneously* for global coupling.

Shnöl [35] has considered an alternate type of global coupling where all oscillators are identically coupled to a medium, which in turn has its own dynamics. Shnöl studied the system

$$\frac{dx^i}{dt}=h(y,x^i)\ , \tag{48a}$$

$$\frac{dy}{dt}=g_0(y)+\frac{\gamma}{N}\sum_{i=0}^{N-1} g_1(y,x^i)\ . \tag{48b}$$

Here the x^i, $i=0,1,\ldots,N-1$, are the oscillator coordinates and y describes the medium. In general $\dim(x^i)\neq\dim(y)$. It is clear that these equations are invariant under arbitrary permutations of the x^i and therefore shift invariance is guaranteed. The synchronization manifold $\mathcal{M}$ is defined by $x^0=x^1=\cdots=x^{N-1}=s(t)$ and $y(t)=y_s(t)$, where $s(t)$ and $y_s(t)$ are determined from the equations

$$\frac{ds}{dt}=h(y_s,s)\ , \tag{49a}$$

$$\frac{dy_s}{dt}=g_0(y_s)+\gamma g_1(y_s,s)\ . \tag{49b}$$

Linearizing (48) about $\mathcal{M}$ one gets

$$\frac{d\xi^i}{dt}=D_xh\xi^i+D_yh\Delta\ , \tag{50a}$$

$$\frac{d\Delta}{dt}=\frac{\gamma}{N}D_xg_1\sum_{i=0}^{N-1}\xi^i+(D_yg_0+\gamma D_yg_1)\Delta\ , \tag{50b}$$

where $\Delta=y-y_s$ and $\xi^i=x^i-s$, and where all Jacobians are evaluated on $\mathcal{M}$. This set of variational equations can be block diagonalized by Fourier transforming the sequence $\{\xi^0,\xi^1,\ldots,\xi^{N-1}\}$, as in Sec. II:

$$\eta^k=\frac{1}{N}\sum_{j=0}^{N-1}\xi^j e^{2\pi ijk/N} \tag{51}$$

(for convenience we have chosen the normalization factor $1/N$ in the Fourier transform). A straightforward calculation yields the transformed variational equations

$$\frac{d\eta^0}{dt}=D_xh\eta^0+D_yh\Delta\ ,$$

$$\frac{d\Delta}{dt}=\gamma D_xg_1\eta^0+(D_yg_0+\gamma D_yg_1)\Delta\ , \tag{52a}$$

$$\frac{d\eta^k}{dt}=D_xh\eta^k,\quad k=1,2,\ldots,N-1\ . \tag{52b}$$

Shnöl arrives at these equations via a different route; the advantage of employing the Fourier transform technique is that the variations η^k have a direct interpretation in terms of spatial modes. The first two equations, (52a), govern variations *within* the synchronization manifold; these equations can also be derived directly from (49). Equation (52b) governs variations *transverse* to $\mathcal{M}$. Stability of the synchronized state is guaranteed provided the Lyapunov exponents of (52b) are all negative. A connection between this synchronization condition and the chaotic synchronization condition discussed in [36,37] can be immediately drawn; the synchronization condition is equivalent to the requirement that the *conditional Lyapunov exponents* of the subsystem (49a) are all negative. Finally, we note that, as in the first global coupling example above, all of the transverse modes lose stability simultaneously.

IV. EXPERIMENTS AND SIMULATIONS

It is important to test the synchronization results discussed above on real physical systems, particularly those

with noise and intrinsic mismatch between the oscillators. This is carried out here for an assembly of coupled chaotic electronic circuits. To facilitate experiments with coupled chaotic oscillators, it was necessary to build a circuit with several desirable properties. First, the circuit was required to exhibit chaos over a large range of parameters, so that weak coupling to other circuits would not immediately destroy the chaotic behavior. Second, the circuit was required to have a single attractor for the parameter region in which it was to be used. Third, the circuit needed to be simple enough that several "identical" oscillators could be easily constructed.

The circuit that was built simulates a modified version of the Rössler equations [38], where the quadratic nonlinearity is replaced by a piecewise linear element and where the "x" equation contains an additional damping term. The basic oscillator is described by the equations

$$\frac{dx}{dt} = -\alpha(\Gamma x + \beta y + \lambda z) , \tag{53a}$$

$$\frac{dy}{dt} \alpha(x + \gamma y) , \tag{53b}$$

$$\frac{dz}{dt} = \alpha[g(x) - z] , \tag{53c}$$

where the function $g(x)$ is piecewise linear, given by

$$g(x) = \begin{cases} 0, & x \le 3 \\ \mu x, & x > 3 . \end{cases} \tag{54}$$

These equations are similar to another set of equations studied independently by Rössler, Hudson, and Rössler [65]. The time factor α is $10^4\,\mathrm{s}^{-1}$ and the other circuit parameters were set to the values $\Gamma = 0.05$, $\beta = 0.5$, $\lambda = 1.0$, $\gamma = 0.133$, and $\mu = 15.0$. Figure 1 shows a schematic of this circuit. Figure 2(a) shows an x-y projection of a chaotic attractor of the circuit for the above parameters. For comparison, Fig. 2(b) shows the same projection generated numerically from Eqs. (53), with the time scaled so that $\alpha = 1$ [66]. The slight disparity between the circuit and the model equations is not bad, considering the large number of resistors with 1% tolerances and the three capacitors with 5% tolerances.

The experimental coupled oscillator configuration consisted of four circuits arranged in a ring, coupled diffusively to nearest neighbors. Three separate experiments were carried out: scalar coupling through the x, y, and z coordinates. We considered y coupling first.

The coupling function $c(y_{i+1} + y_{i-1} - 2y_i)$ was produced by first adding the y signals with operational amplifier adders, then multiplying the resulting sum by the coupling constant c using an analog multiplier chip. The coupling function was then added back into the y equation of the ith oscillator using another operational amplifier adder. With y coupling synchronization was observed for coupling constants $c \ge 0.06$ in time units where $\alpha = 1$. Synchronization was detected in two ways, one qualitative and the other quantitative. The first (qualitative) method was simple visual inspection of oscilloscope traces of the x voltage of one oscillator vs the x voltage of another oscillator for the three pairs (x_0, x_1),

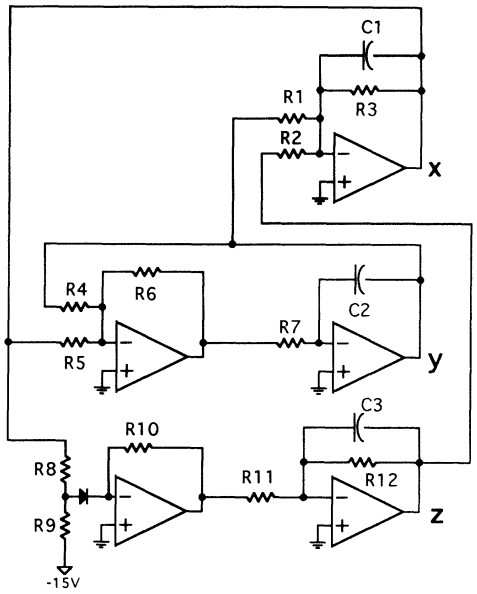

FIG. 1. Schematic of the circuit described by Eqs. (53), the piecewise linear Rössler circuit. The resistor values are $R_1 = 100\ \mathrm{k\Omega}$, $R_2 = 200\ \mathrm{k\Omega}$, $R_3 = 2\ \mathrm{M\Omega}$, $R_4 = 75\ \mathrm{k\Omega}$, $R_5 = 10\ \mathrm{k\Omega}$, $R_6 = 10\ \mathrm{k\Omega}$, $R_7 = 100\ \mathrm{k\Omega}$, $R_8 = 10\ \mathrm{k\Omega}$, $R_9 = 68\ \mathrm{k\Omega}$, $R_{10} = 150\ \mathrm{k\Omega}$, $R_{11} = 100\ \mathrm{k\Omega}$, $R_{12} = 100\ \mathrm{k\Omega}$, $C_1 = C_2 = C_3 = 0.001\ \mu\mathrm{F}$, and the diode is a type MV2101. The operational amplifiers are all type 741.

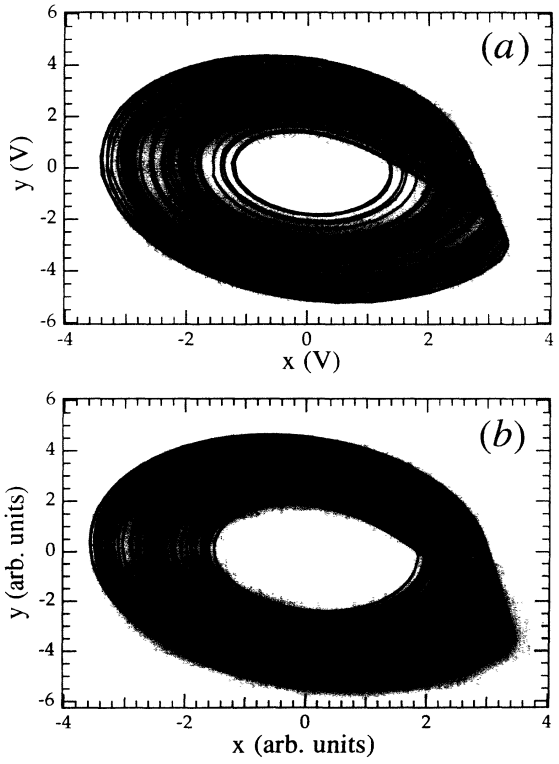

FIG. 2. (a) x-y projection of attractor generated by the piecewise linear Rössler circuit. (b) Same projection for attractor generated from Eqs. (52).

(x_1,x_2), and (x_2,x_3). Quantitatively, the threshold for synchronization was found by measuring the average difference between x voltages of two oscillators before and after a rapid switch in the coupling constant from a large value, such as $c=1.0$, where the oscillators were well synchronized, to a smaller value. Synchronization was considered to be lost when the magnitude of the average difference changed from a small (synchronized) value to a larger offset value. The rate of approach to the offset was observed to be approximately exponential. Faster approach rates were observed as the oscillators were farther from the synchronization threshold. At the synchronization threshold, the average difference between oscillators did not change, and the approach rate to the offset value went to zero.

In the second experiment the four oscillators were coupled in a similar manner through the x variable. In this case synchronization was found for $c\approx 0.05$. Finally, for the z-coupling experiment the oscillators did not synchronize over the entire range of accessible coupling constants.

Figure 3 is a plot of the numerically determined value of the largest transverse Lyapunov exponent for the first ($k=1$) mode, $\lambda^1_{\max}$, versus the coupling constant c, for x, y, and z coupling. In each coupling case $\lambda^1_{\max}$ was found by integrating the $k=1$ variational equations simultaneously with equations (53) and computing the growth rate of a randomly chosen variation. Integration times were $\sim 20\,000$ cycles around the attractor and error bars in the exponents were within the size of the plot symbols. For comparison the numerical value of $\lambda^1_{\max}$ for *vector* coupling is also shown in the plot, along with the corresponding theoretical value computed from Eq. (25). This served as a check of our numerical integration algorithm. The numerical y-coupling threshold $c\approx 0.052$ compares well with the experimental value of $c=0.06$. The numerical x-coupling threshold $c\approx 0.063$ also compares well with the theoretical value of $c\approx 0.05$. Finally, the lack of synchronization in the numerical z-coupling case is consistent with the z-coupling experiment.

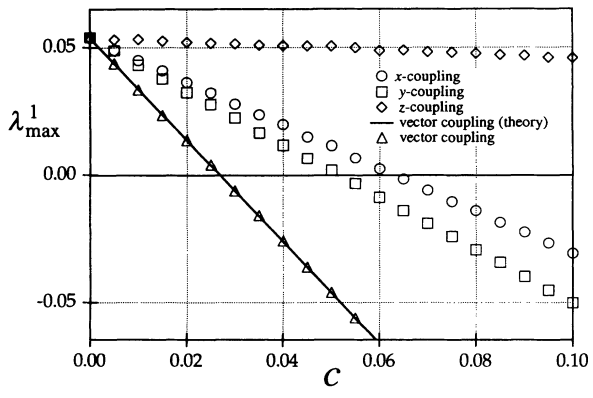

FIG. 3. Largest transverse Lyapunov exponent for x,y,z, and vector coupling for the $k=1$ mode versus coupling constant. Solid line is theoretical vector coupling prediction based on Eq. (25).

Because of experimental limitations on the size of the coupling constant, we were unable to test the large coupling limit theory with the experimental oscillator array. Therefore numerical studies with large coupling constants were carried out. Figures 4(a), 4(b), and 4(c) show $\lambda^1_{\max}$ versus c for a wider range of coupling constants for the x, y, and z coupling cases, respectively. Also shown in each plot is the theoretical large coupling limit prediction for $\lambda^1_{\max}$ obtained from expression (42). In the y-coupling case the agreement between the numerical and theoretical exponents is quite good, even for relatively small coupling constants. Qualitative agreement is seen in the x and z coupling cases. In all cases the large coupling limit theory correctly predicts synchronization or lack thereof as the coupling constant becomes large.

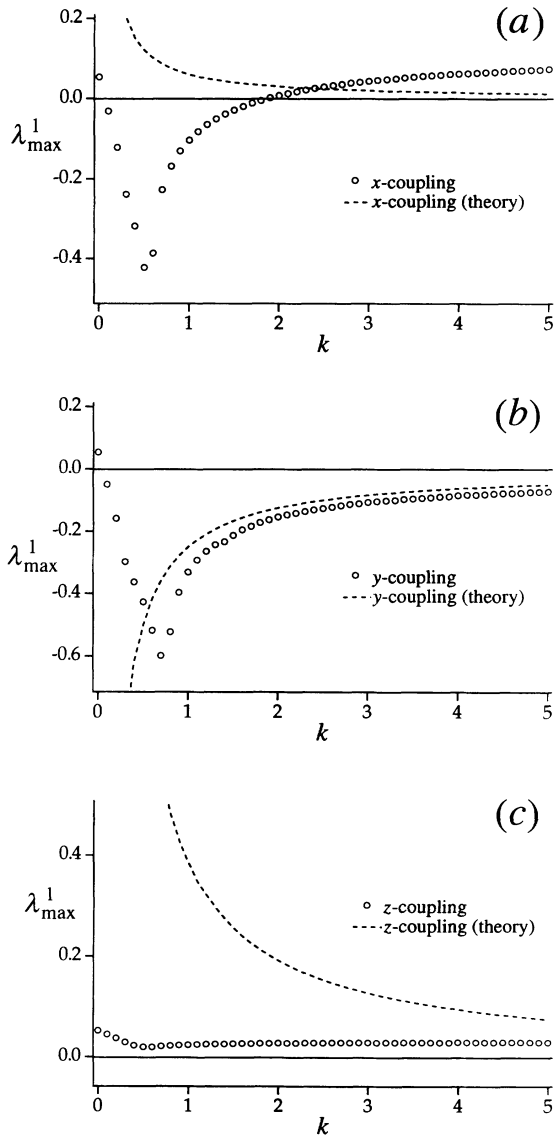

FIG. 4. (a) Largest transverse Lyapunov exponent for the $k=1$ mode and large coupling limit prediction for x coupling as functions of coupling constant. (b) Same for y coupling. (c) Same for z coupling.

Somewhat contrary to expectation is the x-coupling case, which fails to synchronize for large coupling, yet *does* synchronize for smaller coupling constants. A similar phenomenon has been observed in a proportional feedback control technique discussed in a recent paper by Pyragas [67]. This peculiar phenomenon is the topic of ongoing investigations.

V. CONCLUSIONS

A general framework for determining the stability of synchronous chaotic oscillations in coupled oscillator systems with shift-invariant symmetry has been discussed. This framework allows one to systematically reduce a large set of variational equations, governing the stability of the synchronous state, to several independent low-dimensional sets of variational equations. The reduced sets govern the stability of synchronous chaotic (and nonchaotic) behavior and they generally have the same or similar structure. Typically their dimension is that of a single oscillator. The vehicle for carrying out the reduction is the spatial Fourier transform. While this approach is not new, it applies to a large class of coupled oscillator configurations, and thereby groups many previous investigations under one umbrella. The well known cases of nearest-neighbor diffusive coupling and global coupling fall under this umbrella. For cases with scalar diffusive coupling and in the limit of large coupling, an approximate stability criterion for synchronous chaotic behavior has been derived. This criterion is easy to implement (requiring only the average value of the Jacobian on the attractor) and gives useful information without the need for large scale simulations. It is expected to be particularly useful for very large arrays.

Experimental studies of synchronous chaos have been conducted with a set of four diffusively coupled Rössler-like oscillator circuits. Experimental synchronization thresholds for x, y, and z coupling are in good agreement with those found from computed maximal Lyapunov exponents. We conclude that the theoretical synchronization conditions are able to stand up in the presence of realistic noise and in cases where the oscillators are not exactly identical. Finally, maximal Lyapunov exponents for large coupling constants are in good qualitative and reasonable quantitative agreement with theoretical large limit predictions for all scalar coupling configurations.

ACKNOWLEDGMENTS

We would like to thank R. Gilmore, M. Golubitsky, and M. I. Rabinovich for fruitful discussions. J.F.H. is supported by the National Research Council.

APPENDIX: FREE-END ARRAY AS A SHIFT-INVARIANT CASE

Certain coupled oscillators systems that are not in shift-invariant form can be put into that form so the analysis presented in this paper can be applied. Here we carry this out for nearest-neighbor diffusive coupling with *free-end* boundary conditions. The approach is similar to that used to derive equations of motion and stability for coupled systems undergoing Hopf bifurcations [68,69] and for certain cases of motion of vibrations in atomic lattices (cf., [32] and references therein). We see below that the results for chaotic synchronization are the same, and that a more geometric approach can be used to simplify the derivation.

The equations of motion for an array of N diffusively coupled oscillators, $x^i \in \mathbb{R}^n$, with free-end boundary conditions are

$$\begin{aligned}
\frac{dx^0}{dt} &= F(x^0)+c(x^1-x^0)\ , \\
\frac{dx^1}{dt} &= F(x^1)+c(x^2+x^0-2x^1)\ , \\
&\ \ \vdots \\
\frac{dx^{N-1}}{dt} &= F(x^{N-1})+c(x^{N-2}-x^{N-1})\ .
\end{aligned} \tag{A1}$$

The Jacobian on the synchronization manifold is given by

$$J=\begin{bmatrix}
DF-c & c & 0 & 0 & 0 & \cdots & 0 \\
c & DF-2c & c & 0 & 0 & \cdots & 0 \\
0 & c & DF-2c & c & 0 & \cdots & 0 \\
 & \vdots & & & & & \\
0 & \cdots & 0 & 0 & 0 & c & DF-c
\end{bmatrix}, \tag{A2}$$

which does not have a circulant structure. The lack of periodic boundary conditions has changed the first and last equations in Eq. (1) and, as a result, the (0,0), $(0,N-1)$, $(N-1,0)$, and $(N-1,N-1)$ components of the Jacobian have been changed.

We can create the system (A1) and Jacobian (A2) from a shift-invariant system by doubling the size of the system and restricting our interest to a subspace of the doubled system. This is done as follows. The equations of motion for an array of $2N$ diffusively coupled oscillators with periodic boundary conditions are

$$\begin{aligned}
\frac{dx^0}{dt} &= F(x^0)+c(x^1-x^0)+c(x^{2N-1}-x^0)\ , \\
\frac{dx^1}{dt} &= F(x^1)+c(x^2+x^0-2x^1)\ , \\
&\ \ \vdots \\
\frac{dx^{N-1}}{dt} &= F(x^{N-1})+c(x^N-x^{N-1})+c(x^{N-2}-x^{N-1})\ , \\
&\ \ \vdots \\
\frac{dx^{2N-1}}{dt} &= F(x^{2N-1})+c(x^0+x^{2N-2}-2x^{2N-1})\ ,
\end{aligned} \tag{A3}$$

where we have purposely split off the coupling terms in the zeroth and $N-1$st equations. The corresponding Jacobian on the synchronization manifold is

$$K=\begin{bmatrix} DF-2c & c & 0 & 0 & 0 & \cdots & c \\ c & DF-2c & c & 0 & 0 & \cdots & 0 \\ 0 & c & DF-2c & c & 0 & \cdots & 0 \\ & \vdots & & & & & \\ c & 0 & \cdots & 0 & 0 & c & DF-2c \end{bmatrix}, \tag{A4}$$

which has a circulant structure. Note that if we could force $x^{2N-1}=x^0$ and $x^{N-1}=x^N$, we would recover Eqs. (A1) in the first N equations of (A3). The way to do this is shown schematically in Fig. 5; one simply identifies opposite oscillators in the figure. Geometrically, this means we restrict the oscillators to the submanifold defined by $x^{2N-1}=x^0$, $x^{2N-2}=x^1$, etc. This can be carried out by applying a series of 45° rotations to the oscillator coordinates which are to be equated. The result is an overall $2N\times 2N$ transformation matrix of the form

$$T=\frac{1}{\sqrt{2}}\begin{bmatrix} 1 & 0 & \cdots & & 0 & 1 \\ 0 & 1 & \cdots & & 1 & 0 \\ & \ddots & & \iddots & & \\ \vdots & \vdots & 1 & 1 & \vdots & \vdots \\ & & -1 & 1 & & \\ & \iddots & & \ddots & & \\ 0 & -1 & \cdots & & 1 & 0 \\ -1 & 0 & \cdots & & 0 & 1 \end{bmatrix}, \tag{A5}$$

applied to the coordinates in (A3), where all off-diagonal and off-counter-diagonal terms are zero (here 1 denotes the $n\times n$ unit matrix). The matrix in (A5) is orthogonal, hence $T^{-1}=T^t$. Under T the first N coordinates of the new system will satisfy the desired constraints. A straightforward calculation shows that the transformed Jacobian takes the form

$$\tilde{K}\equiv TKT^t=\begin{bmatrix} DF-c & c & 0 & 0 & \cdots & 0 & 0 & 0 & \cdots & & 0 \\ c & DF-2c & c & 0 & \cdots & 0 & \vdots & \vdots & & & \vdots \\ & \vdots & & & & & & & & & \\ 0 & 0 & \cdots & 0 & c & DF-c & 0 & 0 & & & \\ \vdots & & & & 0 & 0 & DF-3c & c & 0 & 0 \cdots & 0 \\ & & & & & 0 & c & DF-2c & c & 0 \cdots & 0 \\ & & & & & & & \vdots & & & \vdots \\ 0 & \cdots & & & & & 0 & 0 & \cdots 0 & c & DF-3c \end{bmatrix}. \tag{A6}$$

Therefore T block-diagonalizes K and the upper block is exactly the Jacobian J of the free-end problem given in (A2).

J itself can be diagonalized by using the fact that the Fourier transform matrix $\mathcal{F}$ diagonalizes K, as discussed in Sec. II,

$$K_{\text{diag}}=\mathcal{F}K\mathcal{F}^{\dagger}, \tag{A7}$$

where $\mathcal{F}^{\dagger}$ is the Hermitian conjugate of $\mathcal{F}$. The "eigenvalues" of K are given by Eq. (23) with $N\to 2N$,

$$q_k=DF-4c\sin^2\left[\frac{\pi k}{2N}\right],\quad k=0,1,\ldots,2N-1. \tag{A8}$$

Let $\phi_k, k=0,1,\ldots,2N-1$, be the corresponding eigenvectors. Then

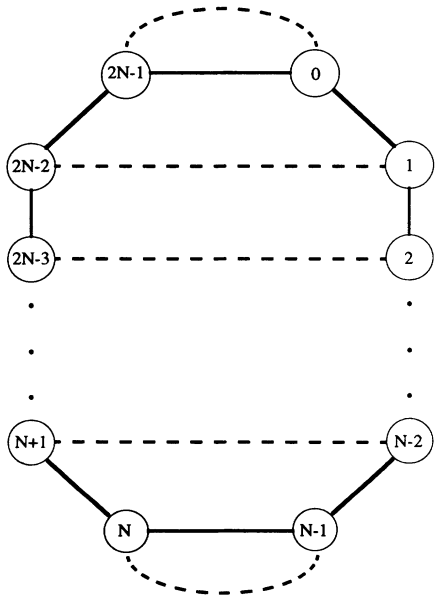

FIG. 5. Diagram of doubled oscillator array. Solid lines represent coupling between the oscillators, while dashed lines represent oscillators that are to be identified through the transformation T.

$$K\phi_k = q_k\phi_k \ ,$$

$$TKT^t(T\phi_k) = q_k(T\phi_k) \ , \tag{A9}$$

$$\tilde{K}(T\phi_k) = q_k(T\phi_k) \ ,$$

which shows that q_k is also an eigenvalue of $\tilde{K}$ with eigenvector $T\phi_k$. Only the first N eigenvalues are associated with the upper block J. Therefore the eigenvalues of J are those in (A8), with $k = 0, 1, \ldots, N-1$, in agreement with Dean's results for matrices occurring in atomic vibration problems [32].

[1] H. G. Winful and L. Rahman, Phys. Rev. Lett. **65**, 1575 (1990).
[2] C. Bracikowski and R. Roy, CHAOS **1**, 49 (1991).
[3] K. Otsuka and J.-L. Chern, Phys. Rev. A **45**, 8288 (1992).
[4] M. Silber, L. Fabiny, and K. Wiesenfeld, J. Opt. Soc. Am. B **10**, 1121 (1993).
[5] Y. Kuramoto, *Chemical Oscillations, Waves, and Turbulence* (Springer-Verlag, New York, 1984).
[6] K. Bar-Eli, Physica D **14**, 242 (1985).
[7] M. Yoshimoto, K. Yoshikawa, and Y. Mori, Phys. Rev. E **47**, 864 (1993).
[8] D. Fisher, Phys. Rev. Lett. **31**, 1486 (1983).
[9] S. H. Strogatz, C. M. Marcus, R. M. Westervelt, and R. E. Mirollo, Physica D **36**, 23 (1989).
[10] A. T. Winfree, *The Geometry of Biological Time* (Springer, Berlin, 1980).
[11] N. Kopell and G. B. Ermentrout, Math. Biosci. **90**, 87 (1988).
[12] G. B. Ermentrout, Physica D **41**, 219 (1990).
[13] R. E. Mirollo and S. H. Strogatz, SIAM (Soc. Ind. Appl. Math.) J. Appl. Math. **50**, 1645 (1990).
[14] J. J. Collins and I. N. Stewart, J. Nonlinear Sci. **3**, 349 (1993).
[15] H. Sompolinsky, D. Golomb, and D. Kleinfeld, Phys. Rev. A **43**, 6990 (1991).
[16] J. M. Kowalski, G. L. Albert, B. K. Rhoades, and G. W. Gross, Neural Networks **5**, 805 (1992).
[17] E. D. Lumer and B. A. Huberman, Neural Comput. **4**, 341 (1992).
[18] H. Nozawa, CHAOS **2**, 377 (1992).
[19] J. C. Alexander, SIAM (Soc. Ind. Appl. Math.) J. Appl. Math. **46**, 199 (1986).
[20] K. Okuda and Y. Kuramoto, Prog. Theor. Phys. **86**, 1159 (1991).
[21] D. Golomb, D. Hansel, B. Shraiman, and H. Sompolinsky, Phys. Rev. A **45**, 3516 (1992).
[22] T. L. Carroll, J. F. Heagy, and L. M. Pecora, Phys. Lett. A **186**, 225 (1994).
[23] I. Waller and R. Kapral, Phys. Lett. **105A**, 163 (1984).
[24] V. S. Afraimovich, N. N. Verichev, and M. I. Rabinovich, Izv. Vyssh. Uchebn. Zaved. Radiofiz **29**, 1050 (1986) [Sov. Radiophys. **29**, 795 (1986)].
[25] N. F. Rul'kov, A. R. Volkovskii, A. Rodríguez-Lozano, E. D. Río, and M. G. Verlarde, Int. J. Bif. Chaos **2**, 669 (1992).
[26] K. Kaneko, Physica D **23**, 436 (1986).
[27] K. Kaneko, Prog. Theor. Phys. **72**, 480 (1984).
[28] G. L. Oppo and R. Kapral, Phys. Rev. A **36**, 5820 (1987).
[29] L. A. Bunimovich and Y. G. Sinai, Nonlinearity **1**, 491 (1988).
[30] W. v. d. Water and T. Bohr, CHAOS **3**, 747 (1993).
[31] H. Fujisaka and T. Yamada, Prog. Theor. Phys. **69**, 32 (1983).
[32] P. Dean, J. Inst. Math. Its Appl. **3**, 98 (1967).
[33] D. E. Rutherford, Proc. R. Soc. Edinburgh **62**, 229 (1947).
[34] D. E. Rutherford, Proc. R. Soc. Edinburgh **63**, 232 (1950).
[35] E. E. Shnöl, Prikl. Mat. Mekh. USSR **51**, 9 (1987).
[36] L. M. Pecora and T. L. Carroll, Phys. Rev. Lett. **64**, 821 (1990).
[37] L. M. Percora and T. L. Carroll, Phys. Rev. A **44**, 2374 (1991).
[38] O. E. Rössler, Phys. Lett. A **57**, 397 (1976).
[39] A. V. Oppenheim and R. W. Schafer, *Discrete-Time Signal Processing* (Prentice-Hall, Englewood Cliffs, NJ, 1989).
[40] I. Pastor, V. M. Peréz-García, F. Encinas-Sanz, and J. M. Guerra, Phys. Rev. E **48**, 171 (1993).
[41] Since the transverse variations are generally complex this statement is technically incorrect, however the real forms of the transverse variations, given by $\chi^k = \frac{1}{2}(\eta^k + \eta^{N-k})$ and $\sigma^k = (1/2i)(\eta^k - \eta^{N-k})$, are transverse to the (real) synchronization manifold $\mathcal{M}$.
[42] J. C. Alexander, I. Kan, J. A. Yorke, and Z. You, Int. J. Bif. Chaos **2**, 795 (1992).
[43] E. Ott, J. C. Sommerer, J. C. Alexander, I. Kan, and J. A. Yorke, Phys. Rev. Lett. **71**, 4134 (1993).
[44] B. R. Hunt (unpublished).
[45] W. H. Press, B. P. Flannery, S. A. Teukolsky, and W. T. Vetterling, *Numerical Recipes, The Art of Scientific Computing* (Cambridge University Press, Cambridge, England, 1990).
[46] C. Cohen-Tannoudji, B. Diu, and F. Laloë, *Quantum Mechanics* (Wiley, New York, 1977).
[47] M. I. Rabinovich (private communication).
[48] A. R. Volkovskii and N. F. Rul'kov, Pis'ma Zh. Tekh. Fiz. **15**, 5 (1989) [Sov. Tech. Phys. Lett. **15**, 249 (1989)].
[49] V. S. Anishchenko, T. E. Vadivosa, D. E. Postnov, and M. A. Safonova, Int. J. Bif. Chaos **2**, 633 (1992).
[50] T. L. Carroll and L. M. Pecora, IEEE Trans. Circuits Syst. **38**, 453 (1991).
[51] T. L. Carroll and L. M. Pecora, IEEE Trans. Circuits Syst. **40**, 646 (1993).
[52] T. Endo and L. O. Chua, IEEE Trans. Circuits Syst. **38**, 1580 (1991).
[53] A. V. Oppenheim, G. W. Wornell, S. H. Isabelle, and K. M. Cuomo, in *Proceedings of the 1992 IEEE International Conference on Acoustics, Speech and Signal Processing* (IEEE, New York, 1992), pp. 117–120.
[54] R. He and P. G. Vaidya, Phys. Rev. A **46**, 7387 (1992).
[55] M. d. S. Viera, P. Khoury, A. J. Lichtenberg, M. A. Lieberman, W. Wonchoba, J. Gullicksen, J. Y. Huang, R. Sherman, and M. Steinberg, Int. J. Bif. Chaos **2**, 645 (1992).
[56] L. O. Chua, L. Kocarev, K. Eckart, and M. Itoh, Int. J. Bif. Chaos **2**, 705 (1992).
[57] N. Gupte and R. E. Amritkar, Phys. Rev. E **48**, 1620 (1993).
[58] K. Cuomo and A. V. Oppenheim, Phys. Rev. Lett. **71**, 65 (1993).

[59] P. Hadley and M. R. Beasley, Appl. Phys. Lett. **50**, 621 (1987).
[60] P. Hadley, Ph.D. thesis, Stanford University, 1989.
[61] D. G. Aronson, M. Golubitsky, and J. Mallet-Paret, Nonlinearity **4**, 903 (1991).
[62] K. Y. Tsang, R. E. Mirollo, and S. H. Strogatz, Physica D **48**, 102 (1991).
[63] K. Y. Tsang and I. B. Schwartz, Phys. Rev. Lett. **68**, 2265 (1992).
[64] M. Tsodyks, I. Mitkov, and H. Sompolinski, Phys. Rev. Lett. **71**, 1280 (1993).
[65] O. E. Rössler, J. L. Hudson, and R. Rössler, Physica D **62**, 80 (1993).
[66] Integrations were carried out with a standard fourth order Runge-Kutta integration algorithm with a fixed stepsize; cf. Ref. [45].
[67] K. Pyragas, Phys. Lett. A **181**, 203 (1993).
[68] I. Epstein and M. Golubitsky, CHAOS **3**, 1-5 (1993).
[69] D. Armbruster and G. Dangelmayr, Math. Proc. Cambridge Philos. Soc. **101**, 167 (1987).

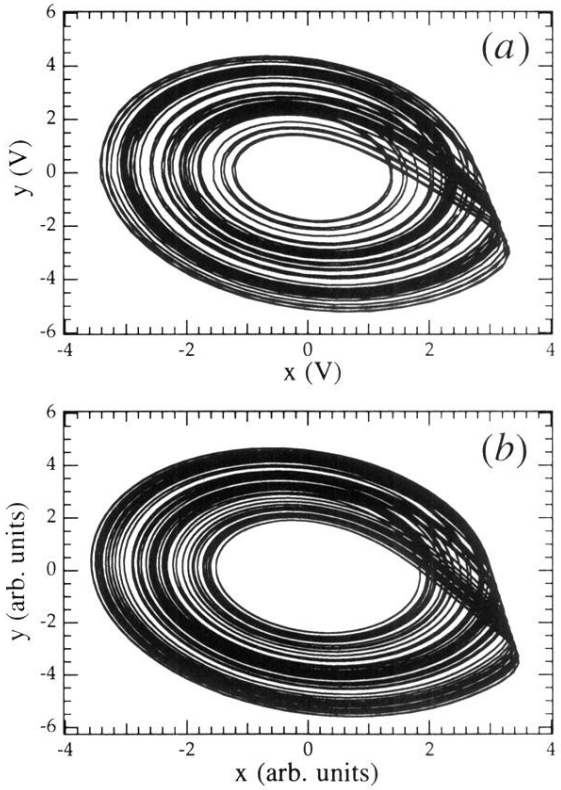

FIG. 2. (a) x-y projection of attractor generated by the piecewise linear Rössler circuit. (b) Same projection for attractor generated from Eqs. (52).